Spots on Adolescent Stars: Remapping DI Herculis with New Techniques

Ryan White* and Dr Benjamin Pope
School of Mathematics and Physics, The University of Queensland, QLD 4072, Australia

Using high cadence time-series photometry from TESS, we fit a state of the art surface map to the primary component of DI Herculis. Our best fit surface map shows two prominent dark spots, similar to previous mappings and chemical clouds on other binaries fit via Doppler imaging. In analysing the residual error of the model, we identify two prominent frequencies in a 3:4 resonance which could feasibly correspond to SpB pulsations. We discuss weaknesses in the model, and suggest future studies of temporal evolution in the spot map, and gravity darkened maps.

Introduction. Low-mass stars are known to have complex surface features, due to magnetic interactions in their upper layers. The cause of this is from charged parcels of hot stellar material moving towards the surface, then subsequently cooling and sinking back down via convective currents [1]. As a result of the spatially varying temperature profile across the convective surface, we would see brighter and darker regions from the hot and cool areas (respectively). The time-series brightness of a star (or lightcurve) would then show dips as these dark star spots come in and out of view while the star rotates on its axis. Several other physical effects can alter the shape of a light curve independently of star spots, including but not limited to: reflection from stellar companions [2], relativistic beaming of the emitted light, and intrinsic stellar variation either from radial pulsation or non-radial acoustic/buoyancy waves.

While the processes that cause star spots in low mass stars are reasonably well constrained, we see this quasiperiodic variability in the lightcurves of some high mass stars, which would suggest star spot activity on their surface. This is problematic, as high mass stars are understood to have radiative outer layers and so convective currents could not explain the observed surface features [3]. There are various examples of early type, chemically peculiar stars that exhibit surface brightness variability which could instead explain these observations. This chemical peculiarity is an ideal scenario, as previous studies have identified isolated 'clouds' of metal gas [4] which would induce photometric and spectroscopic variability.

A considerable proportion of stellar systems (especially those containing high mass stars [5]) are composed of two or more stars, denoted by binary or multiple systems respectively. Understanding the underlying physics of the most extreme of these systems allows us to constrain the phenomena that are relevant to binaries in general. One such extreme binary system is DI Herculis, which Liang et al suggests could host a chemically peculiar primary. DI Her is composed of two closely orbiting, high-mass stars which periodically eclipse each other on a short, $\sim$ 10.5 day orbital period [6]. The fact that this is an eclipsing binary system is significant in being able to uniquely determine a surface map of the primary star (DI Her A). As each star partially occludes the other, we're able to isolate individual surface features which breaks degeneracies in a surface brightness model to the system light curve. Consequently, DI Her serves as an ideal laboratory to investigate peculiar surface features in high mass stars where the physics isn't well understood.

As of writing, the current best fit of a surface model to the DI Herculis system was performed in Liang et al (2022). This involved arbitrarily placing two circular star spots on the surface of the primary star, and sampling from the posterior distribution via a Markov Chain Monte Carlo method [7] for the spot location, radius and uniform brightness property. There is evidence that surface chemical features are not circular [4], which partly explains the systematic inaccuracies in their model evident in the residual flux, especially during the primary eclipse. We note that a well-fitting model during the primary especially is of great importance, as this is when surface features on the primary star can be isolated. We suggest that fitting an analytic light curve to the model using spherical harmonics will yield a far more accurate surface map, especially since so much of stellar physics (such as non-radial stellar pulsations) are described by spherical harmonics.

Methods and Results. The time-series flux data that formed the basis of analysis were obtained from the NASA Transiting Exoplanet Survey Satellite (TESS) [8] via the Barbara A. Mikulski Archive for Space Telescopes (MAST). The two-minute time cadence was necessary for achieving an accurate surface map, as this gave us good time sampling during eclipses. The $\sim$ 27.4 duration of data collection gave us data that spanned more than two orbital periods, including two sets of secondary/primary eclipses . To analyse the data and automatically fit a surface map, we utilised the fast and precise Python package `starry` [9]. The authors describe that they optimise contributions of individual spherical harmonics (up to a user defined degree) in order to analytically fit a surface map given some time-series flux data . In our analysis, we defined a limb-darkening filter degree of 2 (for physical reasons) for both stars, as well as a spherical harmonic map degree of 4 (due to variability in the data and the sampling cadence) for the primary star, DI Her A. Dur-

ing the secondary eclipses, we see minimal deviation from the expected light curve and conclude that DI Her B has (at least to a reasonable precision) a flat surface map. As such, we set the spherical harmonic degree to 1 for the secondary star.

Parameter	Prior	Maximum *a posteriori*
M_A ($M_\odot$)	$5.1 \pm 0.2^\dagger$	5.101
M_B ($M_\odot$)	$4.4 \pm 0.2^\dagger$	4.415
R_A ($R_\odot$)	$2.5 \pm 0.3^\dagger$	2.665
R_B ($R_\odot$)	$2.5 \pm 0.3^\dagger$	2.464
P_A (days)	$1.07 \pm 0.10^\ddagger$	1.075
$P_{\rm orb}$ (days)	$10.55 \pm 0.001^\ddagger$	10.550
i_A (°)	[0, 90]	80.927
$i_{\rm orb}$ (°)	$89.02 \pm 1.0^\ddagger$	88.900
u_1	$0.124 \pm 0.1^\ddagger$	0.106
u_2	$0.262 \pm 0.1^\ddagger$	0.158
$T_{0,B}$ (days)	$2018.4681 + [0, 0.4]^\ddagger$	2018.678
e	[0.50, 0.51]	0.500
ω (°)	$[320.6, 330.6]^\ddagger$	327.286
Ω (°)	90 (fixed)	–

TABLE I. Used priors for the required parameters of the model, as well as our maximum a posteriori values for the fitted parameters. Since the MCMC was not completed in time, we submit the MAP values without variance data. All priors had a bounded normal distribution (≥ 0), except where uniform priors were assumed which are denoted with brackets for their domains. † represents a prior taken from [10], ‡ from [6], and no superscript a mix of both. Some prior variances were arbitrarily inflated so that the model could better explore the parameter space.

We optimised several orbital and stellar properties in the DI Her system to arrive at our fit. The used priors from the literature and maximum a posteriori values are shown in Table I. The vast majority of fit values align within uncertainty of the prior distributions, and significant disagreement is only seen in the limb-darkening coefficients of the stars. The best-fit surface map is shown in Figure 1, and we see two prominent dark regions (somewhat consistent with Liang et al), as well as a brighter region between them. The angular sizes of the surface features are consistent with similar binary systems that exhibit chemically peculiar spots (such as α Andromedae and HD 11753), as seen with high resolution spectra and Doppler imaging [11] [4].

We show the MAP model fit to the time-series data in Figure 2, along with the residual flux across the sampled duration. Even at worst, the residual flux in our model is as low as two thirds that of the model in Liang et al. To truly assess how well our surface map model aligns with the data, we look at the residual flux during the two sets

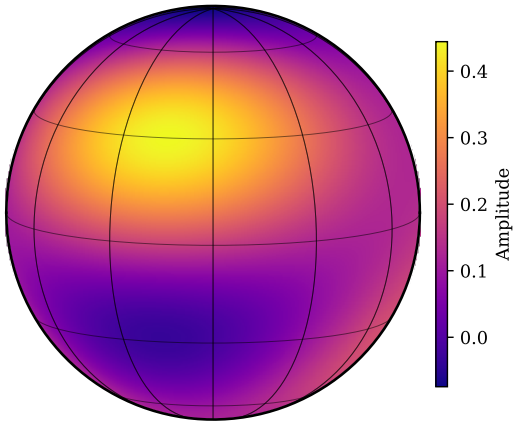

FIG. 1. Best-fit surface map of the DI Her primary star. The inclination is as it appears in the plane of the sky (rotated so that the pole is vertically oriented). The amplitude is in arbitrary units, and is only to show relative brightness of surface features. In actuality, the amplitude is proportional to the true surface brightness, but does not fully represent it. The other side of the sphere mapping is mostly homogeneous in amplitude, and a full, rectangular projection of the mapping is available on the project GitHub repository, as well as an animation of the surface across one rotation.

of eclipses. During eclipses, we see predominately one of the two stars simultaneously with a sliver of the occluded star. As the foreground star optically moves across the surface of the background star, surface features come in and out of view which consequently impacts the observed flux due to their intrinsic brightness. Figure 3 shows the residual flux during each of the 4 observed eclipses, where our model has fit out the bulk of the periodic error and minimised the remaining error significantly. The residuals in both the primary and secondary eclipses are subject to a horizontal shift with respect to the first and second eclipses due to orbital and rotational period misalignment ($P_{\rm orb} = 10.55$ days compared to $10 \times P_A \simeq 10.75$ days). Other inconsistencies in the shape of the residual curves signify time evolution in the surface, which will be addressed in the discussion.

Several seemingly periodic variations in the residuals are seen in Figures 2 and 3. We utilised the `astropy` [12] implementation of the Lomb-Scargle periodogram [13] to show the prominence of periodic behaviour in these residuals, the results of which are shown in Figure 4. We see peaks at the orbital period, at the harmonics of the rotational period of the primary star, and two other main peaks.

Discussion. Even though our `starry` model fit is state of the art, the residuals show that it is still hindered by error intrinsic to the orbital and stellar properties. The most prominent error we see in Figure 4 is due to the rotational period of the primary star, and the harmonics associated with it. We attribute this error mainly to star

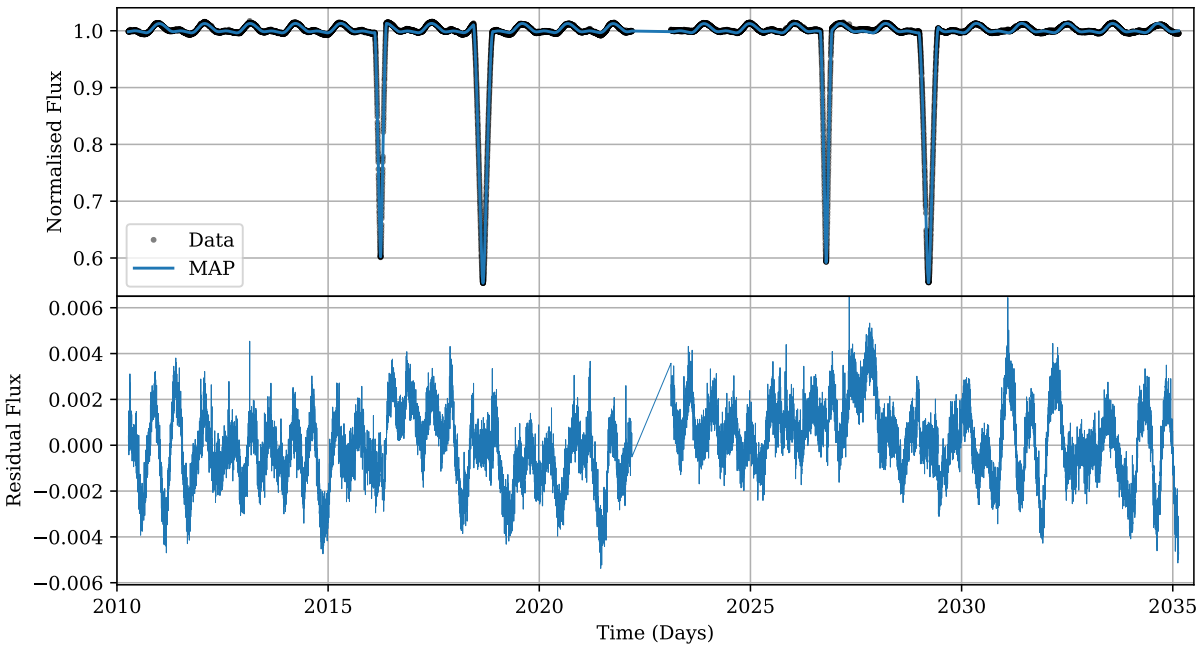

FIG. 2. Top: raw data with the maximum a posteriori fit of the model overlaid in blue. The data were normalised to the median flux value in arbitrary flux units. We see two sets of eclipses, each with a secondary and primary eclipse respectively. The time-series data was obtained from TESS uploads to MAST using the `lightkurve` Python package. Bottom: residuals from the model fit. We see some quasi-periodic oscillations both on short and long time scales (hours to days).

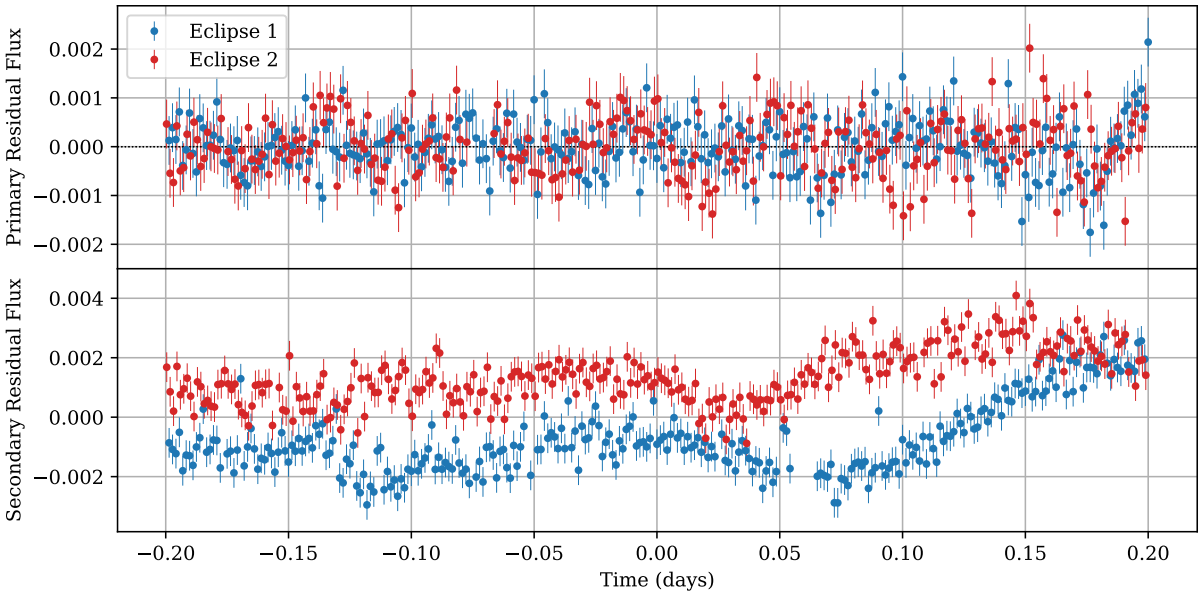

FIG. 3. Residuals of the model during all four eclipses. The time axis represents the time since the minimum brightness of each eclipse. The duration of the primary and secondary eclipses are different, with the primary eclipses occurring from about $-0.2 \leq t \leq 0.2$ days, and the secondary eclipses about $-0.14 \leq t \leq 0.14$ days.

spot modulation over the duration of sampling, and to a lesser contribution limitations in the spherical harmonic model. Modelling spot evolution, perhaps via a linear interpolation between an initial and final spherical harmonic map, might minimise this error. Korhonen et al observed significant spot evolution in a late B type star binary on the order of just a month, and so modelling this time evolution would undoubtedly result in a more accurate fit. As a proof of concept, we fit each half of the TESS data with an independent map, maintaining or-

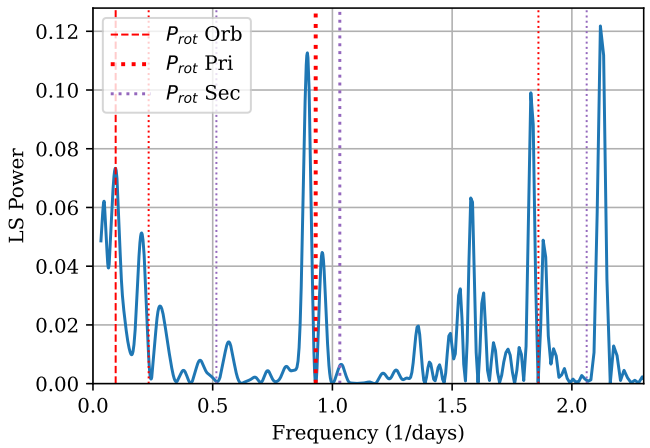

FIG. 4. A Lomb-Scargle Periodogram of the residual flux in the model, in the frequency domain. The dashed line correspond to the peak at the orbital period. The thick red dotted line represents the peak at the primary star rotation period, and the thin red dotted lines harmonics (integer multiples) of this. The purple dotted lines are analogous to the red dotted lines, but for the secondary rotation period found by [6].

bital and stellar properties. The resultant fit minimised much of the error associated with P_A, although it wasn't a rigorous process and was omitted from this study. We also see a strong peak corresponding to the orbital period of the system. Intuitively, we can see this effect in Figure 2, where there is a long-period oscillation that peaks after each secondary eclipse. As this peak occurs when the stars are each moving close to their fastest velocity relative to each other, we propose that this effect could be due to relativistic beaming or a Doppler shift effect. Liang et al dismisses relativistic effects on account of the modelled velocities of the stars, but Doppler effects could be significant as the TESS bandpass is centered in the near infrared [8] and B stars peak in the ultraviolet. Furthermore, this peak is when the stars are closest together in their orbit, and so reflection effects (specifically the primary reflecting off of the secondary) could account for some of the error. Our observations here are consistent with [2], namely with the peak in reflection being close to the secondary minimum in the lightcurve. Aside from the peaks associated with known harmonics, we see two more unexplained peaks at $f \approx 1.6$ and $f \approx 2.1$ days^{-1} that are in an approximate 3:4 resonance. Both of these frequencies could be explained by g-mode pulsations in the interior of one or both stars, as is consistent with Slowly Pulsating B Stars (SpB variables). However, SpB stars are characterised by relatively slow rotation [14] which complicates this. That said, the flux amplitudes of these two frequencies were found to be on the order of ~ 0.05 mag, which matches what we'd expect from SpB variability [14]. In any case, we see evidence of significant time evolution in the former peak via the presence of side lobes about the central frequency. This time evolution could be associated with an unstable g-mode as in [15], consistent with a metallicity of $Z = 0.02$ as was suggested by [16].

Some limitations in our analysis were encountered from both software and time constraints. Firstly, as both of the stars in DI Her are rapidly rotating [6], we would ideally model gravity darkening along the equatorial axis as a result of centrifugal effects. While this is possible under the `starry` implementation, we encountered significant bugs in the output model. While this did impact the accuracy of the model, we expect that this lack of gravity darkening is coupled in the P_A associated error and so was only a part of a $\lesssim 0.2\%$ discrepancy from the data. Similarly, an MCMC analysis of the parameters was not feasible due to time and software constraints. Performing an MCMC in future studies with `starry` is imperative to constrain the orbital and stellar characteristics of the system, especially with a code base as precise as `starry`.

Obtaining high resolution spectra of DI Her, and performing a subsequent Doppler analysis would help show the validity of our fit surface map. As said previously, our fit model is similar to that fit via Doppler techniques in [4], although they were analysing a slowly rotating, late B star. Further analysis is needed to constrain spot properties in rapid rotators like DI Her and other early B stars exhibiting chemical peculiarity and significant magnetism.

Conclusion. Using the fast and precise Python package `starry`, we fit a state of the art surface model to the primary star in the DI Herculis system. The fit was similar with what Doppler techniques have revealed in chemically peculiar stars, which supports our hypothesis that DI Her A might belong to a chemically peculiar or abnormally magnetic class of B star. In analysing the residuals of our model fit, we identified prominent frequencies that are consistent with SpB variable characteristics as in [14] and [15], although this is complicated by the rapidly rotating nature of DI Her A. We proposed modifications to the `starry` package to account for time evolution in a surface model, which we believe would greatly minimise observed error associated with the stellar rotation period. Finally, we expect that similar techniques can be applied to a range of other eclipsing binaries in the TESS catalogue to obtain similarly accurate results for similar systems.

Acknowledgements. Shashank Dholakia was integral in understanding and using the package `starry`, and provided significant help in understanding the underlying physics behind the DI Her system. Some assistance with the University of Queensland HPC, *getafix*, was provided by Jake Moss, for which I am very grateful.

* ryan.white@uqconnect.edu.au

[1] Svetlana V. Berdyugina. Starspots: A key to the stellar dynamo. *Living Reviews in Solar Physics*, 2(1):8, Dec 2005.

[2] L. P. R. Vaz. The Reflection Effect in Eclipsing Binary Systems. *Astrophysics and Space Science*, 113(2):349–364, July 1985.

[3] Bradley W. Carroll and Dale A. Ostlie. *An Introduction to Modern Astrophysics*. Cambridge University Press, 2 edition, 2017.

[4] Korhonen, H., González, J. F., Briquet, M., Flores Soriano, M., Hubrig, S., Savanov, I., Hackman, T., Ilyin, I. V., Eulaers, E., and Pessemier, W. Chemical surface inhomogeneities in late b-type stars with hg and mn peculiarity - i. spot evolution in hd 11753 on short and long time scales. *A&A*, 553:A27, 2013.

[5] Yanjun Guo, Jiao Li, Jianping Xiong, Jiangdan Li, Luqian Wang, Heran Xiong, Feng Luo, Yonghui Hou, Chao Liu, Zhanwen Han, and Xuefei Chen. The Binarity of Early-type Stars from LAMOST medium-resolution Spectroscopic Survey. *Research in Astronomy and Astrophysics*, 22(2):025009, February 2022.

[6] Yan Liang, Joshua N. Winn, and Simon H. Albrecht. DI Herculis Revisited: Starspots, Gravity Darkening, and 3D Obliquities. *The Astrophysical Journal*, 927(1):114, March 2022.

[7] Nicholas Metropolis, Arianna W. Rosenbluth, Marshall N. Rosenbluth, Augusta H. Teller, and Edward Teller. Equation of state calculations by fast computing machines. *The Journal of Chemical Physics*, 21(6):1087–1092, June 1953.

[8] George R. Ricker, Joshua N. Winn, Roland Vanderspek, David W. Latham, Gáspár Á. Bakos, et al. Transiting Exoplanet Survey Satellite. *Journal of Astronomical Telescopes, Instruments, and Systems*, 1(1):014003, 2014.

[9] Rodrigo Luger, Eric Agol, Daniel Foreman-Mackey, David P. Fleming, Jacob Lustig-Yaeger, and Russell Deitrick. starry: Analytic Occultation Light Curves. *The Astronomical Journal*, 157(2):64, February 2019.

[10] Simon Albrecht, Sabine Reffert, Ignas A. G. Snellen, and Joshua N. Winn. Misaligned spin and orbital axes cause the anomalous precession of di herculis. *Nature*, 461(7262):373–376, Sep 2009.

[11] Oleg Kochukhov, Saul J. Adelman, Austin F. Gulliver, and Nikolai Piskunov. Weather in stellar atmosphere revealed by the dynamics of mercury clouds in α andromedae. *Nature Physics*, 3(8):526–529, Aug 2007.

[12] Astropy Collaboration, Adrian M. Price-Whelan, Pey Lian Lim, Nicholas Earl, Nathaniel Starkman, Larry Bradley, David L. Shupe, et al. The Astropy Project: Sustaining and Growing a Community-oriented Open-source Project and the Latest Major Release (v5.0) of the Core Package. *Astrophys. J.*, 935(2):167, August 2022.

[13] William H. Press and George B. Rybicki. Fast Algorithm for Spectral Analysis of Unevenly Sampled Data. *Astrophys. J.*, 338:277, March 1989.

[14] D. W. Kurtz C. Aerts, J. Christensen-Dalsgaard. *Asteroseismology*. Springer Dordrecht, 1 edition, 2010.

[15] Andrea Miglio, Josefina Montalbán, and Marc-Antoine Dupret. Instability strips of slowly pulsating B stars and Beta Cephei stars: the effect of the updated OP opacities and of the metal mixture. *Monthly Notices of the Royal Astronomical Society: Letters*, 375(1):L21–L25, 02 2007.

[16] Claret, A., Torres, G., and Wolf, M. Di herculis as a test of internal stellar structure and general relativity - new apsidal motion rate and evolutionary models. *A&A*, 515:A4, 2010.